# COMPUTATIONAL FLUID DYNAMICS BASED DESIGN AND INVESTIGATION OF NOSE CONE AERODYNAMICS OF FORMULA STYLE STUDENT DESIGNED RACECAR

**3 authors**, including:

Prakhar Mahobia
Indian Institute of Technology Delhi
**1** PUBLICATION   **0** CITATIONS

SEE PROFILE

S . Shukla
Indian Institute of Technology Delhi
**30** PUBLICATIONS   **25** CITATIONS

SEE PROFILE

**Some of the authors of this publication are also working on these related projects:**

Project   Investigation of the Ship Airwakes and its control over the HeloDeck of Naval Ships for Safe Helicopter Operations View project

Project   Investigation of the flow across Isolated Helicopter Rotor View project

**Proceedings of the 1ˢᵗ International and 18ᵗʰ ISME Conference
ISME 18
February 23ʳᵈ – 25ᵗʰ, 2017, NIT Warangal, Warangal**

ISME- TE- 065

# COMPUTATIONAL FLUID DYNAMICS BASED DESIGN AND INVESTIGATION OF NOSE CONE AERODYNAMICS OF FORMULA STYLE STUDENT DESIGNED RACECAR

Dhawal Jain
B.Tech. Student, Dept of Production & Industrial Engg
Indian Institute of Technology, Delhi
Haus Khas, Delhi, India
me2130777@mech.iitd.ac.in

Prakhar Kumar Mahobia
B.Tech. Student, Department of Mechanical Engineering
Indian Institute of Technology, Delhi
Haus Khas, Delhi, India
me1150666@mech.iitd.ac.in

Shrish Shukla
Ph.D. Candidate
Department of Applied Mechanics
Indian Institute of Technology, Delhi
Haus Khas, Delhi, India
amz158347@am.iitd.ac.in

*Abstract* — **In this paper, we present the computational aerodynamics investigation of the nose cone of a Formula Society of Automotive Engineers (FSAE) car. The present work emphasizes on the effect of nose cone design o on the vehicle aerodynamics. The key objective is to minimize the air resistance and obtain significant downforce for better acceleration and traction. The nose-cone shapes inspired from rocketry are selected as viable design options for this study. These shapes are modified based on formula car specifications, tip height, ground clearance and chassis dimensions. The computational study is carried out using the Reynolds-averaged-Navier-Stokes (RANS) turbulence modelling approach with k-epsilon model. Results are presented for the nose-cone geometry variation at certain wind flow conditions. It is concluded that LD Haack-based profile comes out as the best among the alternatives studied. The study tries to demonstrate a method for the geometry selection for aerodynamic features of the car to obtain design efficacy for desired effects by introducing geometric modifications, thus, significantly reducing the air resistance and improve the vehicle aerodynamics.**

## I. INTRODUCTION

Aerodynamics has emerged as an important subject in the recent decades and has profound applications ranging from a ceiling fan to space shuttles. It was in the 60's that the significance of aerodynamics was recognized in motorsports, where studying the flow of air around the vehicle could help in increasing the performance without adding any extra weight. By performance in race cars, we mean reducing the drag or the resistance due to air and increasing the downforce (negative lift)

on the vehicle, which helps in achieving faster accelerations and higher cornering speeds. It has trickled down, and is now employed in the design of passenger and commercial vehicles where aerodynamic drag plays a crucial role in determining the fuel consumption of the car and hence affects its highway performance.

Formula SAE (FSAE), conducted by SAE International, is a student design competition. It was first organized in 1978 and was then known as SAE Mini Indy [1]. In this design competition, college student participate in teams which build small prototype Formula-style race cars. In these events, improving the track performance of the car by reduction of drag is of crucial importance. A reduced drag seriously benefits the car in terms of acceleration and top speed, both of which cater to significant points in the FSAE Competition. The present work is an investigative study of the design of the nose cone employed on the formula style Electric race-car made by the students of the Indian Institute of Technology, Delhi. The primary purpose of this study is to reduce drag on the car, while obtaining some downforce for greater handling and stability.

The work is based on selection of sample shapes from the field of rocketry. Certain shapes from rocketry are selected on the basis of their merit in drag reduction. The primary aim of this work is to obtain favourable low dag conditions. Subsequently, these sample shapes are modified so as to meet the dimensional constraints of the competition as well as make the nose cone shape conformable to the car geometry. These modified shapes are then analysed using steady-state CFD simulations in the ANSYS Fluent 16.2 package. The simulations are done using a pressure based solver with turbulence effects using Reynolds-averaged Navier-Stokes

*To whom correspondence should be addressed. E-mail:* amz158347@am.iitd.ac.in

(RANS) equations with the k-epsilon model (2-eqn) (see Appendix B, (8-14)). The flow conditions are set so as to match the actual conditions as experienced by the car in motion. Due to complexity of the car geometry the simulations are limited to two dimensions. Prior to this, a grid convergence study is performed on a sample shape so as to obtain a reliable grid for actual simulations. Based on simulation results, a shape from the set (chosen earlier from the field of rocketry) having the lowest drag is selected for further investigation.

The selected shape is modified after observing the flow around it so as to direct the flow properly around the top and the bottom surfaces. Upon attainment of satisfactory results, a three dimensional simulation can be performed after adopting the optimized two dimensional geometry for the actual car's three dimensional geometry. The flow parameters for this 3D geometry can be compared with those for the stock body-works to quantize relative performance improvement in terms of drag reduction. The paper ends with presentation of results of the shape comparison study, design modifications to the 2D shape and future scope for study on the optimization of the nose cone or drag reduction on the car.

## II. METHODOLOGY AND WORK

### A. Motivation and Description

The project began with the need of designing an optimal nose cone for a prototype car to be used in the FSAE competition. The main aim of the design was to reduce drag. Since the speeds involved in FSAE rarely reach above 90 km/h, the relative advantage that could be obtained in terms of downforce was not much. As such, most of the design focus was put on designing low drag body features. The ambit of this study was to design a low drag nose cone, and the changes in downforce due to different shapes were not taken into consideration. The nose was designed for an ambient flow speed of V = 20 m/s (72 km/h).

The nose cone is here defined as the region of the body panels that extend from the forward-most point of the car to the front roll hoop in front of the driver. The nose cone thus comprises of 4 major surfaces, viz. the top surface (ending at the front roll hoop), the bottom surface (ending into the under-tray), and the two side surfaces (extends up-to the side impact structure). All these surfaces merge along the edges and at the tip of the nose. This can be further clarified from the Fig. 1 below.

### B. Design Process: Selecting Base Geometry

The first step towards designing the nose cone came from having a starting geometry to work upon for the nose. For this, the field of rocketry was taken into consideration. The field of rocketry demands low drag structures to improve upward acceleration. Moreover, since in rocketry, the focus is not on the generation of downforce from the nose cone, using rocketry based nose cone designs as base shapes for optimization was a justified move. For the work, four main shapes were chosen for
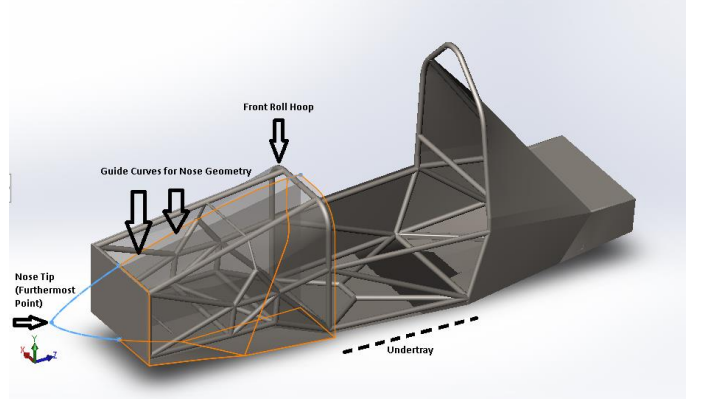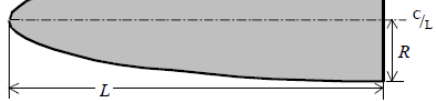


Fig. 1. Nose Cone and related geometry.

optimization. These shapes are LD Haack, LV Haack, Elliptic, and Power-0.5. The equations for the two dimensional cross sectional curves for defining these nose cones can be seen from Table 1.

TABLE 1. ROCKETRY BASED NOSE SHAPES & EQUATIONS



| Name of the shape | Equation |
|---|---|
| Elliptic | $y = R\sqrt{1 - \left(\dfrac{x}{L}\right)^2}$ |
| Power 0.5 | $y = R\left(\dfrac{x}{L}\right)^{0.5}$ |
| LD Haack | $\theta = cos^{-1}\left(1 - \dfrac{2x}{L}\right)$ $y = \dfrac{R\sqrt{\theta - \dfrac{\sin(2\theta)}{2} + \dfrac{\sin^3(\theta)}{3}}}{\sqrt{\pi}}$ |
| LV Haack | $\theta = cos^{-1}\left(1 - \dfrac{2x}{L}\right)$ $y = \dfrac{R\sqrt{\theta - \dfrac{\sin(2\theta)}{2}}}{\sqrt{\pi}}$ |

Out of these four, the elliptic and the power-0.5 curves are based from conic sections geometries. These have been sufficiently validated to perform optimally for certain applications in the domain of rocketry (see [1]). The other two (LD Haack and LV Haack) are cone shapes that were theoretically derived using complex mathematics by Sears-Haack. These curves are based on geometry calculations for minimum drag generation from the nose cone.

## C. Geometric Adaptation and Modifications

Once these cone shapes were selected, the variables in the equations for the shapes were so chosen so as to make the nose cone fit according to the geometry of the chassis and the impact attenuator outline (the nose profile curve must not cut through the chassis and attenuator elements). All this was done in two dimensions. It was so done such that the base of the nose cone lies on the plane of the front roll hoop of the car. This also ensured that the profile departure remains horizontal at the base of the nose cone. This was done so as to have a common uniform flow wake beyond the nose cone, so that only the effects of the shape on the pressure and viscous drag are considered and the drag due to variable flow wakes does not come into the picture. Also the parameters were selected such that the length of the nose from the base to the tip is the same for all (which was in turn decided by the chassis geometry).

Now, the excess part of the geometries was removed from the 2D profiles to account for a modest ground clearance of 50mm. This reduction in the geometry was done by cutting the nose from the bottom region along a straight line starting from the lowermost point of the chassis. Thus, four profiles were obtained for a comparative study of the flow around the nose shape. These changes can be seen in Fig. 2.
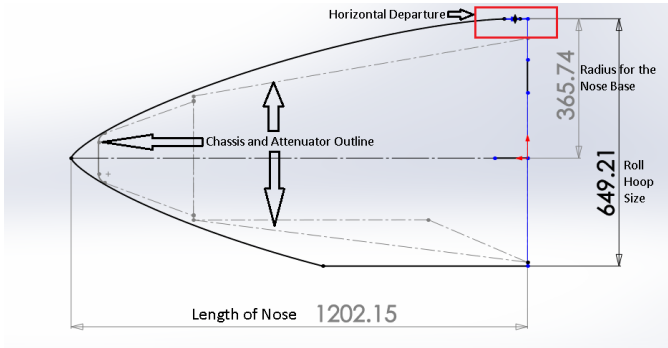


Fig. 2. Nose Cone shape parameters & modifications.

## D. Simulations

The simulations were performed using the ANSYS Fluent FVM solver package. The solver tries to solve the Navier Stokes Equation (see Appendix A, (1-7)) for a variety of fluid flow settings. The characteristic length for the nose was kept at 1.2 meters. With a flow velocity of 20m/s, the characteristic Reynolds Number (1) turns out to be 1.64 x $10^6$.

$$Reynolds\ Number\ (Re) = \frac{\rho VD}{\mu} \qquad (1)$$

The above calculations suggested that the flow around the nose will tend to be turbulent. As such, for the simulations, turbulence models were used.

Turbulence models try to solve the Reynolds Average Navier Stokes (RANS) equation (8-10). There are multiple models that try to solve the RANS equation using certain assumptions. The assumptions for a particular model results in certain set of equations that are derived from the RANS equation on the basis of those assumptions. The lesser the number of equations, the more simplified is the Turbulence Model. For example, the Spalart-Almaras model uses one equation, the k-epsilon (11-14) and the k-omega model uses two equations. The more the number of equations, the more is the complexity of the model, and more is the accuracy of the model, and more is the computational effort required during simulations.

Also, there is a choice of performing the simulations as steady or transient. Transient simulations lead to additional time terms in the characteristic equations and are solved using time marching approach. These are often required when our flow is expected to change with time in space. Steady simulations are performed for those cases when the time variability of the flow can be ignored. Our work pertains to steady state simulations around the nose cone of the car.

Before the comparative study, a grid convergence study was performed on the elliptic nose cone profile. This grid convergence study was performed using ANSYS Fluent Package with a Double Precision Serial Solver using k-e models. All simulations were done using k-epsilon steady state solver model. In this study, the meshing was first done at a coarse level. The simulation results on the Coefficient of Drag were observed for this mesh. The mesh was then successively made finer until the results did not vary with increased fineness of the mesh. Finally, an appropriate mesh (as summarised in Table 2) was selected.

Analysis was performed in the ANSYS Workbench Software Package with the Fluid Flow (Fluent) analysis system. The mesh was made using the Workbench interface of the project package with ICEM CFD as the background meshing software. The computational domain is selected so as to sufficiently capture the flow physics. A too large a computational domain will lead to excessive computational requirements, whereas a too small a computational domain will result in inability to take into account the flow physics of wakes/ flow turning, wake turbulence etc. which affect the overall aerodynamics of the car. The computational domain was selected so as to have 2L in the front, 4L behind, 1.5H from the top and 50mm Ground Clearance around the nose body. Here, L is the length of the nose (fixed by chassis geometry and FSAE Rules to 1200 mm). The computational domain was further divided in the vertical direction as depicted in Fig. 3-4. This division was done so as to make the mesh coarser in the relatively unaffected region of the flow and hence reduce the node count and hence shorten simulation run time. The summary of the mesh (obtained from the grid convergence study) is given in the Table 2. The Inflationary mesh was selected so as to have the dimension perpendicular to the surface of the immediate volume element next to the surface as the $y+1$ thickness of the boundary layer. The y+ thickness was computed using online tools [2] and is based on the values of the Reynolds Number, the Flow Velocity, the Geometry and …

| Category | Description / Value | | |
|---|---|---|---|
| Geometry | Overall Length of Nose | | 1200 mm |
| | Base Radius of Nose (Horizontal Departure) | | 365 mm |
| | Nose Tip Height from the Road | | 335 mm |
| Computational domain (see Fig. 3) | Ahead from tip of nose | | 2L |
| | Behind from rear of Nose | | 4L |
| | Vertically above the highest point on the nose | | 1.5H |
| | Below the nose cone (Ground Clearance) | | 50 mm |
| | Partition Line (Above highest point on nose) | | 0.5H |
| Mesh Summary (see Fig. 4) | Method | | Quad dominant |
| | Region A Element size | | 20 mm |
| | Region B Element size | | 10 mm |
| | Edges of the Nose Element size | | 0.5 mm |
| | Inflationary Mesh around the nose body | Final Element Ratio | 0.8 |
| | | Growth Rate | 1.25 |
| | | Number of Layers | 15 |
| Setup and Solution | Analysis Type | | 2 D |
| | Precision | | Double |
| | Serial/Parallel Solver | | Serial |
| | Pressure/ Density Based | | Pressure Based (As the flow is well below sonic) |
| | Steady/Transient | | Steady |
| | Model | | K-epsilon (Standard) |
| | Boundary Conditions | Inlet | Velocity Inlet, 20m/s, Turbulence Intensity 1% & 0.6 Hydraulic Dia. |
| | | Road | Moving Wall, 20m/s horizontal translational velocity |
| | | Body | Stationary Wall |
| | | Outlet Rear | Pressure Outlet, Turbulence Intensity 1% & 0.65m Hydraulic Dia. |
| | | Outlet Top | Pressure Outlet, Turbulence Intensity 1% & 0.65m Hydraulic Dia. |
| | Reference Values | | Computed from Input |
| | | | Over all Zones |
| | Monitors | | Cd on Body |
| | | | Cl on Body |
| | | | Residuals: made to converge to 0.001 |
| | Solution Methods | | SIMPLE Solver with Second Order Upwinded Momentum and Second Order Upwinded Turbulence Kinetic Viscosity |
| | Solution Controls | | Lowered Under Relaxation Factors for **p** and TKE, Later changed to default values when solution starts to converge |
| | Number of Iterations | | Until Convergence if converges successfully |
| | | | 10,000 if does not converge but becomes steady |
| | | | Solved again with different settings if no convergence |

other aspects. With this kind of mesh size and computational domain, the mesh is expected to have around (1.6 x $10^5$ nodes and 1.8 x $10^5$ elements)
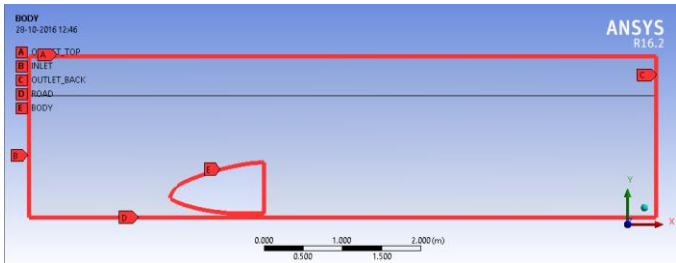

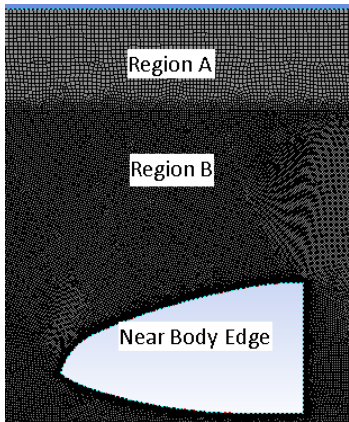Fig. 3: Computational Domain and Boundaries


Fig. 4: Meshing in different regions.

For the comparative study, the CFD analysis was performed in ANSYS Fluent using a double precision solver and steady state simulations with k-epsilon turbulence models. Table 2 summarises the settings for the analysis.

*E. Results of Comparative Study*

The Comparative Study was performed with taking the drag coefficient as the parameter to be optimised. As the simulations were done only on the 2D nose profile and not on the entire 3D assembled CAD of the car, the absolute values of the drag calculated does not make sense. However, relative performance of the nose cones in terms of drag reduction can be clearly be judges based on the relative values of the drag coefficients. The results suggested that the LD Haack Profile was the optimal among the four alternatives chosen. The results can be seen from the Table 3.

TABLE 3: RESULTS OF THE COMPARATIVE STUDY

| Profile | Fx (Newton) | Fy (Newton) | Cd |
|---------|-------------|-------------|------|
| LD Haack | 71.25 | 323.98 | 0.447 |
| Power 0.5 | 112.34 | 435.16 | 0.705 |
| Elliptic | 99.66 | 365.45 | 0.626 |
| LV Haack | 131.38 | 421.17 | 0.825 |

The results of the comparative study suggested that the LD Haack Profile served best for our purpose. As such, this geometry was chosen and further investigation of the flow patterns on this geometry was performed to optimise the shape for drag reduction. Incidentally, this profile also gave the lowest amount of lift, showing its merit for being better than other curves in downforce generation.

The next phase of the design process involved observing the flow patterns various contours of the fluid flow (static pressure, velocity magnitude, turbulence, etc.). One of these contour graphs can be seen below.
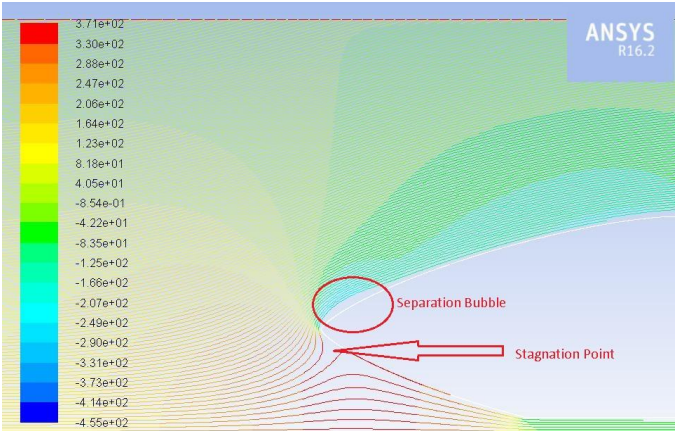

Fig. 5: Path-lines colored by pressure variation

One striking feature that was seen from the pressure contours and the velocity contours was the occurrence of a stagnation point not at the tip of the nose cone, but somewhat below that. Due to this, unwanted lift was being generated along with increased drag force.

### III.    CONCLUSION AND FUTUTRE SCOPE

With this paper, a first approach to design of aerodynamic features of race-cars was demonstrated with the conclusion of LD Haack based profiles being better than the other alternatives considered. However, as aerodynamic effects are highly sensitive to curvature changes, generalization of results has to be done with utmost care. For the work of this paper, one can conclude that the LD Haack profile can be used as the base geometry for aerodynamic design of the nose cone for the application presented in the paper.

With the observation of the stagnation point and the separation bubble in the LD Haack profiled nose, the future scope of the project includes changes in the geometry in order to eliminate these adverse effects. A lower nose may serve to eliminate the adverse stagnation point and the separation bubble. This would require certain approximations and assumptions while altering the shape of the nose to get a lower nose. Ultimately, this design will be an iterative process where new geometries may expose further complexities in the flow. The final goal can be to adapt the two dimensional geometry to the 3D features of the car

5

chassis and perform 3D simulations to get a truer picture of the flow patterns and the aerodynamic performance.

<div align="center">REFERENCES</div>

[1] Ashley Van Milligan, "*Drag of Nose Cones*", PEAK OF FLIGHT Newsletter ISSUE 346, Aug 27, 2013, Apogee Components Inc., www.apogeerockets.com.

[2] Pointwise Yplus Calc., www.pointwise.com/yplus/

[3] Francesco Mariani, Claudio Poggiani, Francesco Risi, Lorenzo Scappaticci, "*Formula- SAE Racing Car: Experimental and Numerical Analysis of External Aerodynamics*", 69th Conference of the Italian Thermal Machines Engineering Assn. ATI2014.

[4] Sneh Hetawala, Mandar Gophane, Ajay B.K., Yagnavalkya Mukkamala, "*Aerodynamic Study of Formula SAE Ca*r", 12th Global Congress on Manufacturing and Management, 2014.

[5] Doig, G. and Beves, C. (2014) "*Aerodynamic design and development of the Sunswill IV solar racing car*", Int. J. Vehicle Design, Vol. 66, No. 2, pp.l43-167.

[6] Ponnappa Bheemaiah Meederira, "*Aerodynamic development of an IUPUI Formula SAE specification car with Computational Fluid Dynamics (CFD) analysis*", Indiana- University, Purdue- University. Indianapolis.

[7] Satyan Chandra, Allison Lee, Steven Gorrell and C. Greg Jensen, "*CFD Analysis of PACE Formula-1 Car*", Computer-Aided Design & Applications, PACE (1), 2011, 1-14 © 2011 CAD Solutions, LLC, DOI: 10.3722/cadaps.2011.PACE.1-14.

[8] Gary A. Crowell Sr., "*The Descriptive Geometry of Nose Cones*", © 1996 Gary A. Crowell Sr.

<div align="center">APPENDIX</div>

*A. Navier Stokes Equations for an Incompressible flow*
The continuity equation:

$$\frac{\partial \rho}{\partial t} + div(\rho \boldsymbol{u}) = 0; \quad (2)$$

X-momentum (similarly for other directions):

$$\frac{\partial(\rho u)}{\partial t} + div(\rho u \boldsymbol{u}) = -\frac{\partial p}{\partial x} + div(\mu\ grad\ u) + S_{M_x}; \quad (3)$$

Internal energy:
$$\frac{\partial(\rho i)}{\partial t} + div(\rho i \boldsymbol{u}) = -p\ div\ \boldsymbol{u} + div(k\ grad\ T) + \Phi + S_i; \quad (4)$$

And, equations of state

$$p = p(\rho, T)\ and\ i = i(\rho, T). \quad (5)$$

For a perfect gas, $\quad (6)$
$$p = \rho RT\ and\ i = C_v T.$$

Here, Φ is the dissipation function and accounts for the viscous stresses in the internal energy equation.

$$\Phi = \mu \left\{ 2\left[ \left(\frac{\partial u}{\partial x}\right)^2 + \left(\frac{\partial v}{\partial y}\right)^2 + \left(\frac{\partial w}{\partial z}\right)^2 \right] + \left(\frac{\partial u}{\partial y} + \frac{\partial v}{\partial x}\right)^2 + \left(\frac{\partial u}{\partial z} + \frac{\partial w}{\partial x}\right)^2 + \left(\frac{\partial v}{\partial z} + \frac{\partial w}{\partial y}\right)^2 \right\} + \lambda(div\ \boldsymbol{u})^2. \quad (7)$$

*B. Turbulence modelling and rans*

For turbulence modelling, the flow variables can be decomposed into their mean and fluctuating components. The instantaneous value is written with a lowercase letter, its mean is denoted by an uppercase letter, and the fluctuating part is given by a lowercase letter with a prime symbol after the letter. Thus,

$$\boldsymbol{u} = \boldsymbol{U} + \boldsymbol{u'}, \quad (8)$$

The continuity equation becomes
$$\frac{\partial \rho}{\partial t} + div(\rho \boldsymbol{U}) = 0. \quad (9)$$
The momentum equation changes to (x-momentum)
$$\frac{\partial(\rho U)}{\partial t} + div(\rho U \boldsymbol{U}) = -\frac{\partial P}{\partial x} + div(\mu\ grad\ U) + \left[ -\frac{\partial(\rho \overline{u'^2})}{\partial x} - \frac{\partial(\rho \overline{u'v'})}{\partial y} - \frac{\partial(\rho \overline{u'w'})}{\partial z} \right] + S_{M_x}. \quad (10)$$
Similar equations for momentum in the y and the z direction can be written.
For the k-e equations:
The instantaneous kinetic energy of the flow is the sum of the mean flow kinetic energy and the turbulent flow kinetic energy
$$k(t) = K + k, \quad (11)$$
Where
$$K = \frac{1}{2}(U^2 + V^2 + W^2) \quad (12)$$
And
$$k = \frac{1}{2}(u'^2 + v'^2 + w'^2). \quad (13)$$
Now,
$$e_{i,j}(t) = E_{i,j} + e'_{i,j}. \quad (14)$$
Here, $e_{i,j}(t)$ is the instantaneous rate of deformation of a fluid element in a turbulent flow. Governing equations for *k* and *e* are of the form:

$$\begin{aligned} &(Rate\ of\ change\ term) \\ &+ (Transport\ by\ convention) \\ &= (Transport\ by\ diffusion) \\ &+ (Rate\ of\ production) \\ &+ (Rate\ of\ destruction) \end{aligned} \quad (15)$$

<div align="center">6</div>